ALMA memo 450 - 21mar2003

Heterogeneous Imaging with the ALMA Compact Array

M. C. H. Wright

Radio Astronomy laboratory, University of California, Berkeley, CA, 94720

ABSTRACT

The ALMA Compact Array will be a powerful telescope at sub-millimeter wavelengths for imaging the large scale structures which are not well sampled by ALMA. In this memo, we propose an observing mode for the ACA as a heterogeneous array of 7 and 12 m antennas. We compare three compact configurations: the ACA (12 x 7 m), a heterogeneous ACA with 4 x 12 m antennas, and the most compact ALMA configurations with 60 x 12 m antennas.

We present tables of the synthesised beam FWHM, brightness sensitivity and sidelobe levels for source declinations +30, 0 and −30 degrees. Using the ACA as a heterogeneous array with four 12 m antennas doubles the collecting area of the ACA and provides synthesised beams and brightness sensitivities which fill a useful parameter space between the ACA alone and the most compact configurations of the ALMA telescope. Heterogeneous observing provides more short spacings and a good cross calibration of the 7 and 12 m antennas.

Calibration of the bandpass and polarization characteristics can be improved by scheduling a few more 12 m antennas for the ACA at times when these calibrations are needed. The location of the ACA in relation to the ALMA array, and the correlator configuration should be considered with these possibilities.

1. Introduction

The ALMA Compact Array (ACA) is being designed to provide short spacing and single dish data for the ALMA array. The current plan is for twelve 7 m antennas to provide short spacing interferometer data, and four 12 m antennas to provide single dish data and additional sensitivity for calibrating the 7 m interferometer array. In this memo we explore the imaging properties of the ACA using the 7 and 12 m antennas together in a heterogeneous array. This heterogeneous array is very similar to compact configurations for the CARMA array with nine 6.1 m and six 10.4 m antennas. The ACA 7 m antenna diameters are 15.4% larger than the 6.1 m antennas, and the ALMA 12 m antenna diameters are 14.8% larger than the 10.4 m antennas. Thus, we expect that the imaging properties of the ACA heterogeneous array are very similar to those of the CARMA array with an observing frequency 15% higher, or a source size 15% smaller. The imaging properties of the CARMA array are discussed in BIMA memo 91.

In this memo we present simulations for the ACA using simple PYTHON scripts to control MIRIAD tasks. The scripts are similar to those used in ALMA memo 428 simulations, but are slightly more complex because of the different antenna sizes used in the heterogeneous ACA telescope, and use more flexible PYTHON scripts instead of CSH.

2. Simulations

For this memo, we generate uv-data for a point source with thermal and atmospheric phase noise, do a phase calibration, and make an image and beam. A Gaussian fit is made to the synthesised beam, and the results written into a table. The brightness sensitivity, beam FWHM, and residual sidelobe level after the fit are calculated. Timing information for each step is given. The script takes $\sim$ 10s run time on a PC or laptop.

Figure 1 shows a trial ACA configuration with 12 x 7 m antennas and 4 x 12 m antennas. The 7 m antennas are arranged in two nested Reuleaux triangles (see Keto, 1997). The 12 m antennas are placed asymetrically outside the Reuleaux triangles to give an approximately Gaussian uv sampling with as many short spacings as possible without excessive synthesised beam sidelobes or antenna shadowing. This configuration was optimized using Boone's code (Boone 2001) with a target Gaussian FWHM=40m for the uv distribution. Other configurations should be explored. For example, a hexagonal close packed configuration offers the most short spacings; the high sidelobes can be reduced by randomizing and optimizing. Logarithmic spirals offer a central high density of uv samples with an approximately Gaussian uv distribution providing good beam sidelobes. For comparison, some logarithmic spiral and ring configurations were evaluated for the 15-antenna CARMA telescope in BIMA memo 91.

The simulations exclude all antenna shadowing which was calculated from the projected uv spacing. In a heterogeneous array with different antenna structures, shadowing depends on the height and relative placement of the 7 and 12 m antennas and cannot be calculated simply from the projected uv spacing. In practice, flagging the shadowed data is probably best done on-line from a model of the antenna structure and configuration. Each configuration was sampled from HA -2 to $+2$ hours, with an elevation limit of 10 degrees. We used natural weighting of the uv-data with a double sideband receiver temperature 80 K, an atmospheric model with zenith opacity 0.08 at 230 GHz, and a bandwidth 8 GHz. Cross correlations are made between all antennas. Assuming an aperture efficiency of 60%, we used antenna gains of 40, 120, and 70 Jy per K for the 12, 7, and cross correlations between 12 and 7 m antennas respectively. The weighting and sensitivities were calculated from the resulting system temperatures and antenna gains. Placing the larger antennas at the longest radii in the array configurations provides a more uniform sensitivity in the uv data, and reduces the required uv data sample rate ($\delta uv = D/2\lambda$, where D is the antenna diameter).

3. Results

We compare 4 compact configurations: (1) the ACA (12 x 7 m antennas), (2) the heterogeneous ACA with 4 x 12 m antennas, (3) the ALMA compact configurations 1 and 2 with all uv spacings, and (4) the ALMA compact configurations with uv spacings tapered to a FWHM=40 m and a maximum spacing of 48m to match the ACA heterogeneous configuration.

Table 1 lists the synthesized beam FWHM, sensitivity $RMS[\mu Jy]$ and $T_b rms[\mu K]$, sidelobes levels (% RMS, Max & Min), and fraction of the data remaining after shadowed data are omitted, Nvis[%], for each configuration and source declinations +30, 0 and −30 deg. The heterogeneous ACA with an 8 hour track is also listed to show the effects of larger hour angles (the last 3 rows in Table 1).

3.1. Sensitivity

The collecting area of the heterogeneous ACA with 4 x 12 m antennas $\sim$ 2x that of the ACA alone (12 x 7 m antennas) as seen in the RMS point source sensitivity. The synthesized beam area $\sim$ 2x that of the ACA alone, so the brightness sensitivity is about the same, even though the resolution is increased. For comparison, the most compact configurations of the ALMA telescope give about the same brightness sensitivity at $\sim$ 4x the resolution. When convolved to the $\sim 4.5''$ resolution of the heterogeneous ACA, the ALMA configurations 1 and 2 have about 4x the brightness sensitivity, and use $\sim$ 25% of the uv data. If one is interested in source structures larger than λ/D, where D is the antenna diameter, then the ACA, and the heterogeneous ACA with 4 x 12 m antennas nicely extend the range of spatial frequencies sampled by interferometer measurements with about the same brightness sensitivity.

3.2. uv Sampling

Figures 2–4 show the uv coverage for a heterogeneous with 12 x 7 m and 4 x 12 m antennas for declination +30, 0, and −30 degrees. The uv tracks from the correlations of the different sized antennas are intermixed, allowing good cross calibration of the 7 and 12 m antennas. The uv coverage is reasonably complete from the 7 m central hole to about 25 m, with an approximately Gaussian distribution with a FWHM = 40 m. The sampling shown is for HA from −2 to +2 hours. Extending the HA coverage from −4 to + 4 hours give better uv coverage, in particular completing the uvtracks down to the 7 m antenna shadowing from all directions, but suffers from more antenna shadowing and higher system temperatures at low elevations (see Table 1). More closely packed antenna configurations may give more short spacings, but suffer from more antenna shadowing, and higher sidelobes.

3.3. Calibration

Table 2 gives the sensitivity per baseline for each combination of 7 and 12 m antennas assuming 60% aperture efficiency, Tsys=200 K, and 1 minute integration. The table lists the sensitivity per baseline for calibrating the antenna gains (amplitude and phase) in an 8 GHz bandwidth, the bandpass with a 1 MHz spectral resolution, and the brightness sensitivity at $5''$ angular resolution at 230 GHz. For antenna based calibration, the RMS is reduced by the *sqrt* of the number of reference antennas (i.e. a factor $\sim 2 - 4$). The calibration sensitivity is greatly enhanced by using correlations with 12 m antennas. This is especially useful for calibration of the bandpass and instrumental polarization for the 7 m antennas at sub-millimeter wavelengths where strong calibrators are hard to find.

Usually, the bandpass and polarization calibrations are slowly time variable and need only be made at infrequent intervals. The signal to noise can be greatly improved by allocating more 12 m antennas to the ACA array for these calibrations. This can readily be done within the framework of dynamic scheduling. The ACA can be thought of as a sub-array with special characteristics (mixed antenna sizes, perhaps with nutating subreflectors on some of the antennas to enhance the single dish observing). More 12 m antennas can be allocated to the ACA for bandpass and polarization calibration observations. Antennas which are closer to the ACA may suffer from less atmospheric phase fluctuations, so the location of the ACA in relation to the ALMA array, and the requirements for the correlator should be considered with these possibilities.

4. Conclusions

A heterogeneous observing mode for ACA has $\sim$ twice the sensitivity of the ACA alone, and will be a powerful telescope at sub-millimeter wavelengths for imaging the large scale structures which are not well sampled by ALMA. If one is only interested in sensitivity at *uv* spacings greater than $\sim$ 12 m, then the ALMA configurations with 60 x 12 m antennas clearly provide much greater sensitivity. The design of the ACA configuration is a compromise between antenna shadowing and the most short spacings. Heterogeneous observing provides a useful mode for ACA observations. ALMA is much more sensitive, so the focus should be on getting short spacings to complement ALMA. Heterogeneous observing provides more short spacings and a good cross calibration of the 7 and 12 m antennas. The signal to noise for bandpass and polarization calibrations can be greatly improved by allocating more 12 m antennas to the ACA array for these calibrations. This can readily be done within the framework of dynamic scheduling. The location of the ACA in relation to the ALMA array, and the configuration for the correlator should be considered with these possibilities.

5. Acknowledgements

I thank Peter Teuben for converting the CSH scripts to PYTHON scripts including writing a number of python procedures which can be reused. Thanks also to Frederic Boone for providing his configuration optimization code, and help with its use for these compact configurations.

6. References

"Interferometric array design: Optimizing the locations of the antenna pads", Frederic Boone, 2001, A&A 377, 368.

"The shapes of cross-correlation Interferometers", Eric Keto, 1997, ApJ, 475, 843

"Miriad Users Guide", 1999, Bob Sault & Neil Killeen, http://www.atnf.csiro.au/computing/software/miriad

"Compact Configuration Evaluation for CARMA", Melvyn Wright, BIMA memo 91, http://bima.astro.umd.edu/memo/memo.html

"Compact Configuration Evaluation", Melvyn Wright, ALMA memo 428, http://www.alma.nrao.edu/memos/index.html

Table 1: Compact Configurations

Config	DEC	$RMS[\mu Jy]$	Beam [arcsec]	$T_b rms[\mu K]$	Sidelobe[%]:RMS	Max	Min	Nvis[%]
ACA	-30	95	6.34 x 5.02	69	2.3	15.3	-10.3	100
ACA	0	99	6.60 x 5.21	67	3.6	43.3	-14.3	99
ACA	30	174	9.02 x 4.97	90	3.2	21.2	-12.9	50
ACA+4	-30	48	4.41 x 4.11	61	2.1	15.7	-9.5	100
ACA+4	0	50	4.68 x 4.20	59	3.3	32.9	-14.0	99
ACA+4	30	75	6.72 x 4.01	64	2.6	18.4	-11.5	60
config1	-30	6	1.63 x 1.47	58	0.5	2.6	-5.0	100
config1	0	6	1.64 x 1.59	53	0.7	6.1	-4.6	100
config2	30	8	1.61 x 1.55	74	0.6	4.1	-4.3	89
config1 4.5″	-30	15	4.47 x 4.40	18	1.5	10.6	-13.0	23
config1 4.5″	0	15	4.52 x 4.48	17	1.8	12.6	-12.2	25
config2 4.5″	30	20	4.50 x 4.40	23	1.3	13.1	-12.2	22
ACA+4 8h	-30	37	4.65 x 4.20	44	1.5	11.2	-8.9	91
ACA+4 8h	0	40	4.72 x 4.37	45	2.7	32.6	-12.0	79
ACA+4 8h	30	67	6.39 x 4.19	58	2.3	14.2	-12.0	39

Table 2: Sensitivity per baseline

Antennas	Equivalent diameter	JyperK	RMS (8 GHz)	RMS in 1 MHz	RMS in 5”
m x m	m	Jy/K	[mJy]	[Jy]	[K]
12 x 12	12	41	9	0.8	0.8
12 x 7	9.2	70	16	1.5	1.3
7 x 7	7	120	28	2.5	2.3

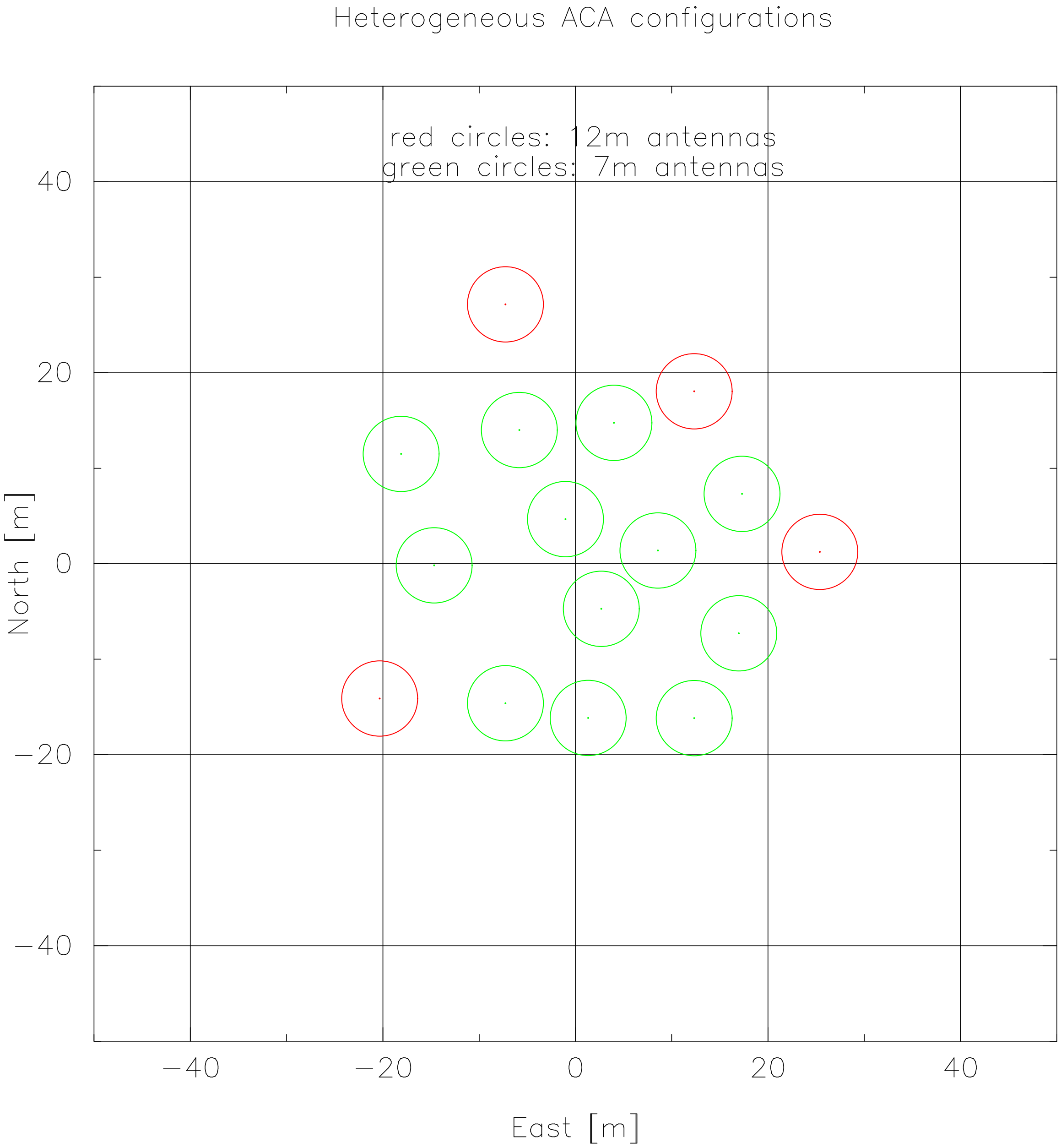

Fig. 1.— Heterogeneous ACA configurations. The larger symbols show the positions of the 12 m antennas.

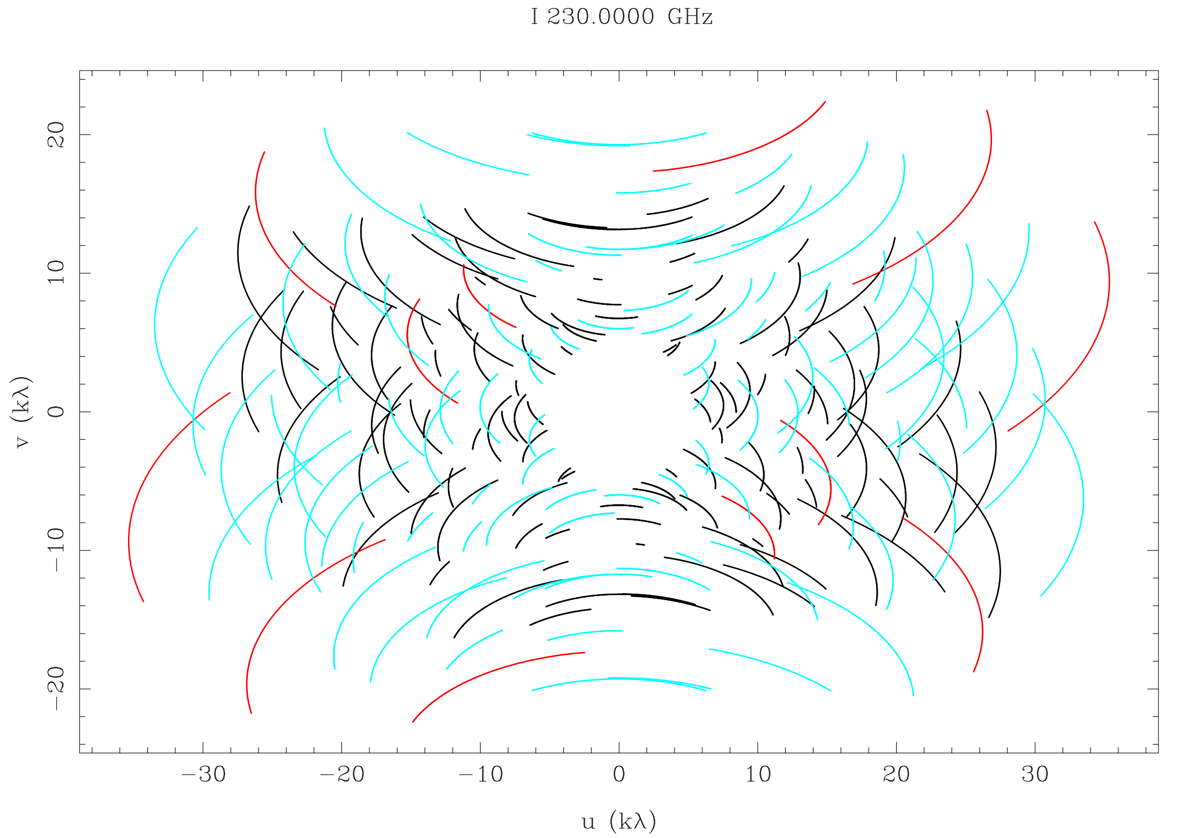

Fig. 2.— *uv* coverage for heterogeneous Alma Compact Array with 12 x 7 m and 4 x 12 m antennas at declination +30 deg. The *uv* data were sampled from HA −2 to +2 hours. 12 m x 12 m correlations in red, 7 m x 7 m in black, and 7 m x 12 m in blue.

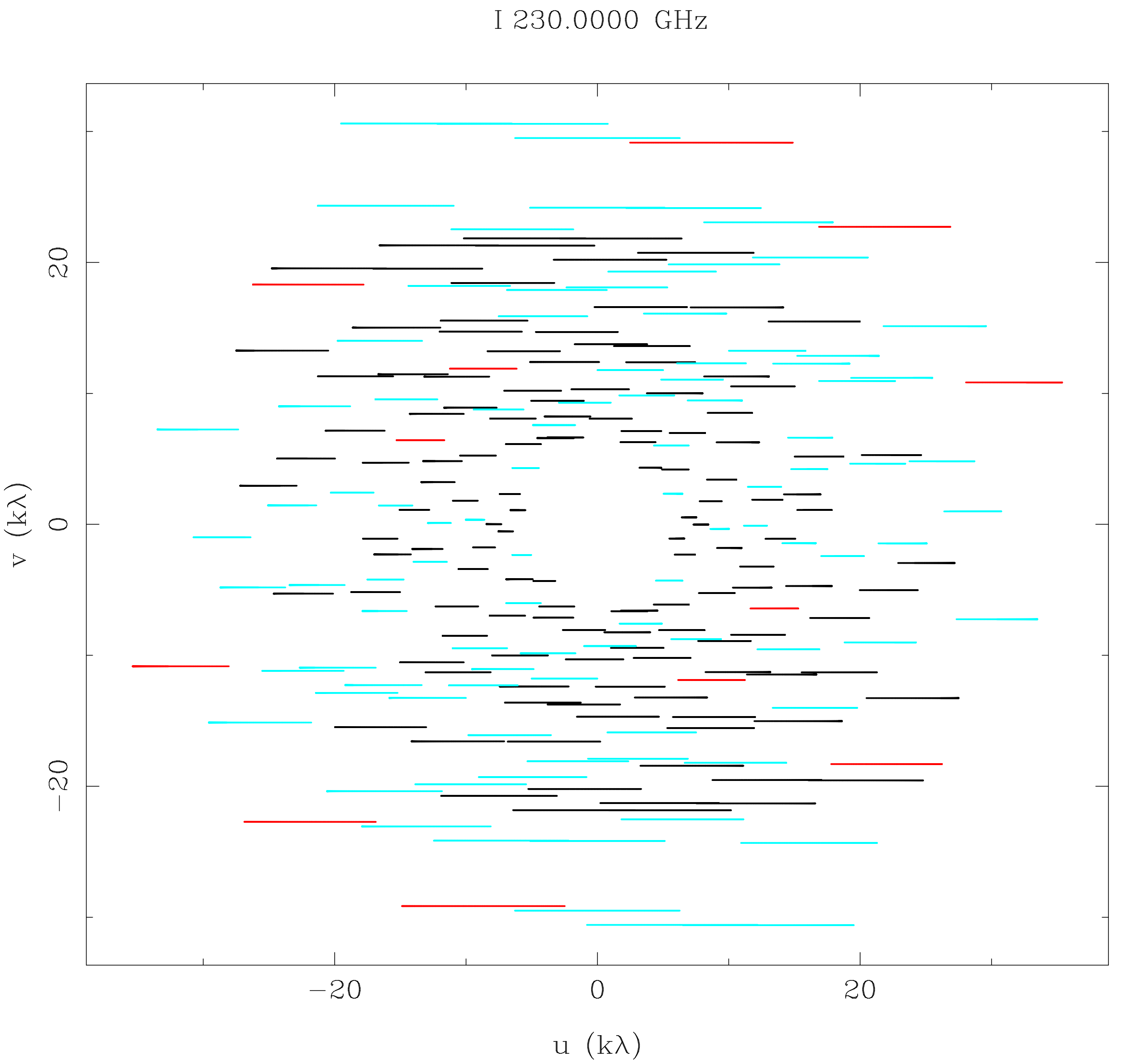

Fig. 3.— *uv* coverage for heterogeneous Alma Compact Array with 12 7 m and 4 12 m antennas at declination 0 deg. The *uv* data were sampled from HA −2 to +2 hours. 12 m x 12 m correlations in red, 7 m x 7 m in black, and 7 m x 12 m in blue.

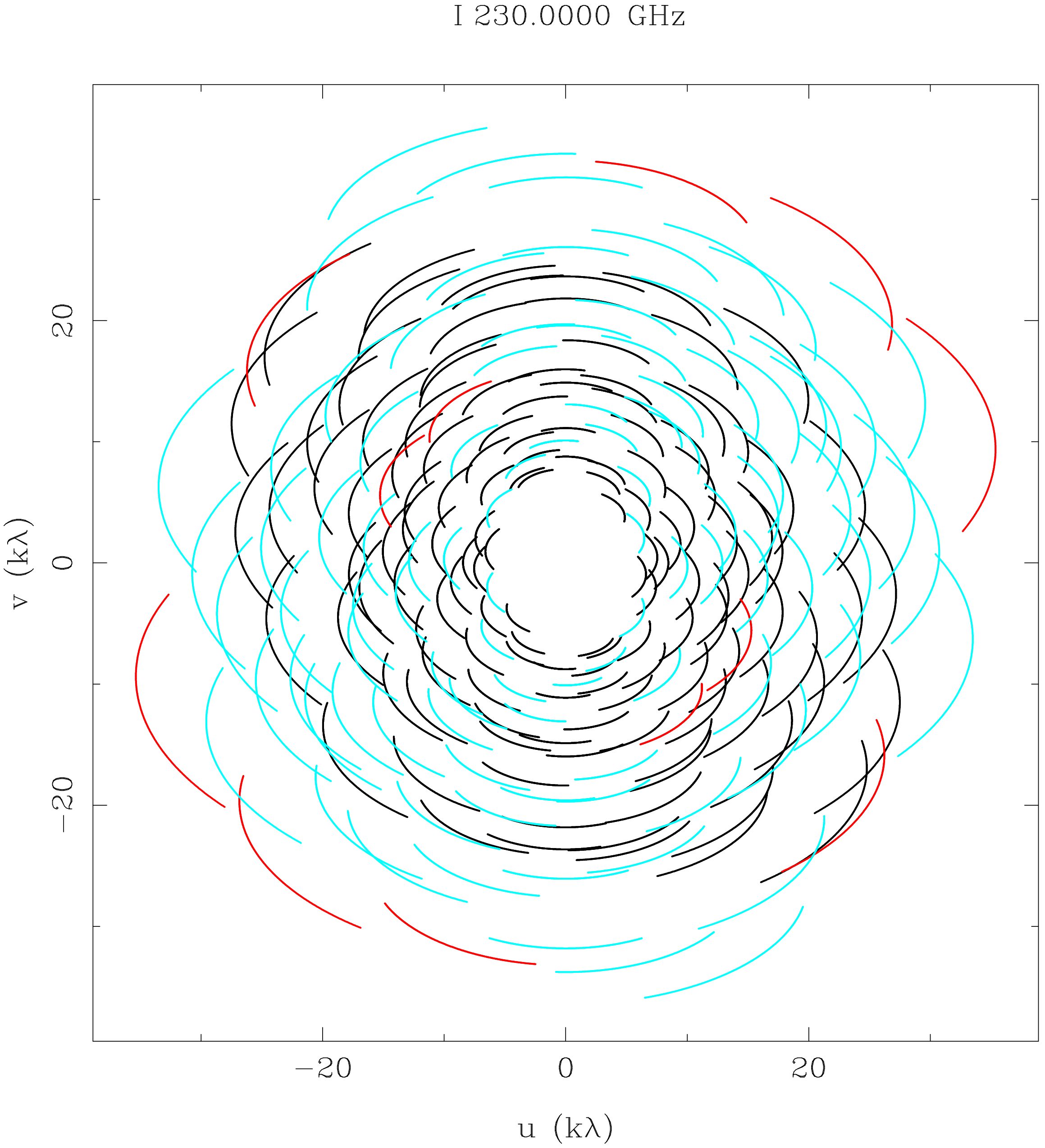

Fig. 4.— *uv* coverage for heterogeneous Alma Compact Array with 12 7 m and 4 12 m antennas at declination −30 deg. The *uv* data were sampled from HA −2 to +2 hours. 12 m x 12 m correlations in red, 7 m x 7 m in black, and 7 m x 12 m in blue.